

Theoretical study on electronic spectra and aurophilic attraction in $[\text{Au}_3(\text{MeN}=\text{COMe})_3]_n$ ($n = 1-4$) complexes

Fernando Mendizabal ^{a,*}, Benjamín Aguilera ^b, Claudio Olea-Azar ^b

^a Departamento de Química, Facultad de Ciencias, Universidad de Chile, Casilla 653, Santiago, Chile

^b Departamento de Química Inorgánica y Analítica, Facultad de Ciencias Químicas y Farmacéuticas, Universidad de Chile, Casilla 233, Santiago 1, Chile

Abstract

The aurophilic attraction and the spectroscopic properties of $[\text{Au}_3(\text{MeN}=\text{COMe})_3]_n$ ($n = 1-4$) were studied at the MP2 and density functional theory (B3LYP and PBE) levels. Theoretical calculations at the MP2 level are in agreement with experimental geometries and aurophilic attraction, and to a lower extent for PBE. The absorption spectra of these gold(I) complexes were calculated by the single-excitation time-dependent (TD) density functional method. All complexes showed MMCT and MLCT transitions interrelated with the gold-gold intermolecular distance. The values obtained at the PBE level are in agreement with the experimental range.

1. Introduction

Gold(I) complexes having intra- and intermolecular gold-gold interactions have been synthesized and characterized, and their absorption-emission spectra have been studied in detail [1-5]. Experimentally, the mono- and binuclear Au(I) compounds show strong $^1(5d\sigma^* \rightarrow 6p\sigma)$ transitions in the UV-visible region attributed to a singlet-singlet transition assigned to a ligand to metal-metal bond charge transfer (LMMCT). The $5d\sigma^*$ assignment is referred to the antibonding combination of $5d_{z^2}(\sigma^*)$ orbitals, and the $6p\sigma$ to the bonding combination $6p_z$ orbitals [6,7]. In general, their luminescent properties are highly diversified, ranging from metal-centered (MC), metal-to-ligand charge transfer (MLCT) to intraligand charge transfer (ILCT) transitions [8].

When in the complexes studied there are two or more gold atoms, they show evidence of aurophilic interactions. At the theoretical point of view, the aurophilic attraction is considered as a correlation effect, strengthened by relativis-

tic effects, this phenomenon can be accounted [9,10]. Closed-shell aurophilic interactions ($d^{10}-d^{10}$) are estimated to be energetically similar to hydrogen bonds (20-50 kJ/mol) [10]. The mechanism behind such attraction is the dispersion (van der Waals) interaction, with additional allowance for virtual charge transfer terms [11]. The optical properties of molecules can be calculated from CIS and higher levels [12,13]. However, recently the predicting power of density functional theory (DFT) with the time-dependent (TD) approach makes it the method of choice. There have been several reports of excellent agreement with experimental absorption and emission spectra in different gold complexes [14-17].

A gold complex that presents both intra- and intermolecular aurophilic interactions and has been structural and spectroscopically well characterized is the trimeric organometallic complex $[\text{Au}_3(\text{MeN}=\text{COMe})_3]$ [18-20]. In the solid state the minimal unit shows an individual molecule of the planar trigold complex (Fig. 1). The intramolecular Au-Au distance is 330.8 pm. The individual molecules form a columnar structure whose intermolecular Au-Au distance is 334.6 pm [18]. When the crystals dissolve in a solvent like chloroform, acetone or toluene, the structure is destroyed, and only single minimal units exist in solution. This is

* Corresponding author. Fax: +56 2271 3888.

E-mail address: hagua@uchile.cl (F. Mendizabal).

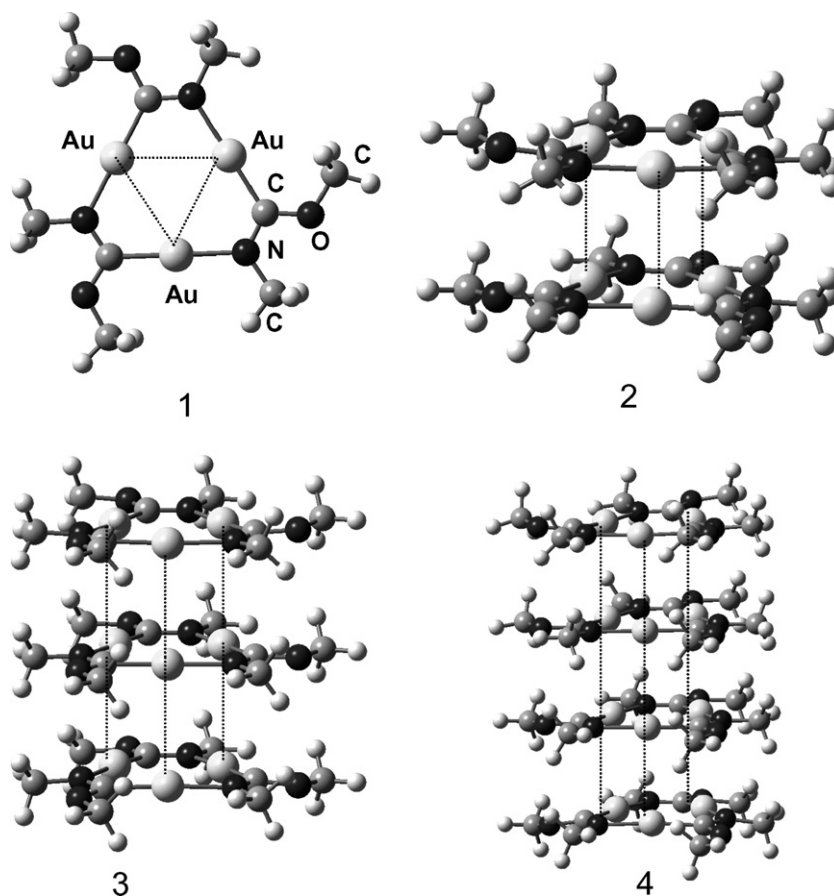


Fig. 1. The $[\text{Au}_3(\text{CH}_3\text{N}=\text{COCH}_3)_3]_n$ ($n = 1-4$) models (1-4).

reflected in the spectroscopic properties, because in the solid state the complex shows an excited band at 380 nm, while the absorption spectrum of a chloroform solution shows three bands at 250, 265, and 285 nm [18,21].

There are two complete theoretical studies centered on the minimal unit of the $[\text{Au}_3(\text{MeN}=\text{COMe})_3]$ triangular gold complex and on the electronic structures and luminescent properties at the MP2, CIS and B3LYP levels [22,23]. The absorption and emission spectra show reasonable

agreement with the experimental results in the solution phase.

The aim of the present work is to study theoretically the $[\text{Au}_3(\text{MeN}=\text{COMe})_3]_n$ ($n = 1-4$) complexes and relate the results to their excitation spectra. We propose to study the effect of several complexes and how their interactions can influence the spectroscopic absorption properties. To our knowledge, so far no systematic TD-DFT research has been made on these systems.

Table 1
Main geometric parameters of the $[\text{Au}_3(\text{CH}_3\text{N}=\text{COCH}_3)_3]_n$ ($n = 1-4$) systems (distances in pm and angles in degrees)

System	Method	Au–Au ^a	Au–Au ^b	AuN	AuC	CN	OC	CO	NAuAu
$[\text{Au}_3(\text{CH}_3\text{N}=\text{COCH}_3)_3]_1(\text{C}_s)$	MP2	321.0		204	196	146	134	142	61.28
	B3LYP	337.8		209	202	147	134	142	59.07
	PBE	334.9		208	200	146	135	143	59.48
$[\text{Au}_3(\text{CH}_3\text{N}=\text{COCH}_3)_3]_2(\text{C}_1)$	MP2	317.3	325.0	204	195	146	134	142	63.70
	B3LYP	339.0	480.0	209	201	146	134	142	58.63
	PBE	335.0	363.0	208	199	146	135	142	61.31
$[\text{Au}_3(\text{CH}_3\text{N}=\text{COCH}_3)_3]_3(\text{C}_s)$	B3LYP	339.0	430.7	209	210	146	135	142	59.75
	PBE	335.0	384.3	208	200	146	135	142	59.28
$[\text{Au}_3(\text{CH}_3\text{N}=\text{COCH}_3)_3]_4(\text{C}_1)$	B3LYP	338.0	405.5	209	210	136	135	142	59.60
	PBE	338.3	369.3	208	199	146	135	142	59.30
$[\text{Au}_3(\text{CH}_3\text{N}=\text{COCH}_3)_3]_n$	Exp.	330.8	334.6	203	200	148	136	143	59.70

^a Au–Au intramolecular distance within each molecular unit.

^b Au–Au Intermolecular distance between neighboring molecular units.

2. Models and methods

The $[\text{Au}_3(\text{MeN}=\text{COMe})_3]_n$ ($n = 1-4$) models used in our study are depicted in Fig. 1. The geometries were fully optimized at the scalar relativistic MP2 ($n = 1, 2$), B3LYP and PBE (Perdew–Burke–Ernzerhof) [24] levels in the gas phase. The MP2 calculation requires a large computational effort and was only used on models **1** and **2**. With respect to the latter method, it has been used in the study of weak interactions [25,26]. It is the best available functional for dispersion forces, without parameters fitted to experimental data. However, none of the existing functionals are optimal for evaluating the largely dispersed aurophilic based contribution [27].

The excitation energies were obtained at the B3LYP and PBE levels by using the time-dependent perturbation theory approach (TD-DFT) [28,29], which is based on the random-phase approximation (RPA) method [30]. The TD-DFT calculations do not evaluate the spin–orbit splitting, and the values are averaged.

Table 2

Interaction energies, $V(R_e)$, in kJ/mol, with BSSE for the $[\text{Au}_3(\text{CH}_3\text{N}=\text{COCH}_3)_3]_2$ model

Method	Au–Au	$V(R_e)$	Au–Au pair
HF ^a	325	+101.3	+33.8
MP2	325	−75.9	−25.3
PBE	363	−5.3	−1.8
B3LYP	480	+12.6	+4.2

Au–Au intermolecular distances in pm.

^a MP2 geometry is used.

The calculations were done using the TURBOMOLE package (version 5.8) [31]. For Au, the 19 valence-electron (VE) quasi-relativistic (QR) pseudo-potential (PP) of Andrae et al. [32] was employed. We used two f-type polarization functions on gold ($\alpha_f = 0.20, 1.19$) [10]. Also, the C, O and N atoms were treated through PPs, using double-zeta basis sets with the addition of one d-type polarization function [33]. For the H atom, a double-zeta basis set plus one p-type polarization function was used [34]. For MP2 and

Table 3

TD-DFT/PBE singlet-excitation calculations for $[\text{Au}_3(\text{CH}_3\text{N}=\text{COCH}_3)_3]_n$ ($n = 1-4$)

System	λ_{calc} (nm)	f^a	λ_{exp} (nm)	Contribution ^b	Transition type
$[\text{Au}_3(\text{CH}_3\text{N}=\text{COCH}_3)_3]_1$	301	0.0351	285	71a' → 74a'' (33)	MLCT (s + dz ² → π*)
	273	0.1814	265	72a' → 73a'' (30)	MLCT (s + dz ² → π*)
				71a' → 75a'' (35)	MMCT (s + dz ² → s + p)
				69a'' → 73a'' (16)	LLCT (π → π*)
	254	0.1033	250	69a'' → 76a'' (16)	LLCT (π → π*)
				70a'' → 76a'' (43)	MLCT (s + d → π*)
69a'' → 76a'' (17)				LLCT (π → π*)	
68a'' → 74a'' (11)				LLCT (π → π*)	
$[\text{Au}_3(\text{CH}_3\text{N}=\text{COCH}_3)_3]_2$	349	0.1586	380	144a → 146a (47)	MLCT (s + dz ² → π)
				143a → 145a (43)	MLCT (s + dz ² → π)
$[\text{Au}_3(\text{CH}_3\text{N}=\text{COCH}_3)_3]_3$	370	0.3089	380	215a' → 218a'' (51)	MLCT (s + dz ² → π)
				216a' → 217a'' (42)	MLCT (s + dz ² → π)
$[\text{Au}_3(\text{CH}_3\text{N}=\text{COCH}_3)_3]_4$	405	0.4099	380	287a → 290a (51)	MLCT (s + dz ² → π)
				288a → 289a (41)	MLCT (s + dz ² → π)

^a Oscillator strength.

^b Values are $|\text{coeff.}|^2 \times 100$.

Table 4

TD-DFT/B3LYP singlet-excitation calculations for $[\text{Au}_3(\text{CH}_3\text{N}=\text{COCH}_3)_3]_n$ ($n = 1-4$)

System	λ_{calc} (nm)	f^a	λ_{exp} (nm)	Contribution ^b	Transition type
$[\text{Au}_3(\text{CH}_3\text{N}=\text{COCH}_3)_3]_1$	263	0.0533	285	72a' → 74a'' (32)	MLCT (s + dz ² → π*)
	250	0.07649	265	71a' → 73a'' (30)	MLCT (s + dz ² → π*)
				72a' → 75a'' (88)	MMCT (s + dz ² → s + p)
				69a'' → 73a'' (3)	LLCT (π → π*)
230	0.2320	250	71a'' → 73a'' (33)	MLCT (s + d → π*)	
			69a'' → 74a'' (29)	LLCT (π → π*)	
$[\text{Au}_3(\text{CH}_3\text{N}=\text{COCH}_3)_3]_2$	272	0.1668	380	144a → 146a (42)	MLCT (s + dz ² → π)
				143a → 147a (37)	MLCT (s + dz ² → π)
$[\text{Au}_3(\text{CH}_3\text{N}=\text{COCH}_3)_3]_3$	287	0.3094	380	216a' → 218a'' (38)	MLCT (s + dz ² → π)
				215a' → 217a'' (34)	MLCT (s + dz ² → π)
$[\text{Au}_3(\text{CH}_3\text{N}=\text{COCH}_3)_3]_4$	290	0.4080	380	287a → 290a (40)	MLCT (s + dz ² → π)
				288a → 289a (35)	MLCT (s + dz ² → π)

^a Oscillator strength.

^b Values are $|\text{coeff.}|^2 \times 100$.

PBE, the efficient resolution of the identity (RI) approximation was employed to obtain the final geometry and make the calculation feasible [35].

3. Results and discussion

3.1. Molecular geometry and auriphilic energies

We have fully optimized the geometries for the $[\text{Au}_3(\text{MeN}=\text{COMe})_3]_n$ ($n = 1-4$) models (**1-4**). Table 1 shows the main parameters, together with relevant experimental structural data. The theoretical results are in agreement with the experimental data when compared within each $[\text{Au}_3(\text{MeN}=\text{COMe})_3]$ unit. It is seen that the struc-

tural parameters change from the B3LYP or PBE to the MP2 level in models **1** and **2**. The usual correlation-induced shortening is found for all systems, suggesting auriphilic attractions. This is clearly due to the effect of the ligands that remain joined to the gold atoms in the basic units.

This situation changes drastically when we compare the closest Au–Au intermolecular distances of the neighboring units ($n = 2-4$). In the case of $n = 2$, an attraction at the MP2 level is produced. The distance obtained with the MP2 method is the shortest (325 pm). It is worth noting that the MP2 approximation overestimates the metallic interactions [8,10]. On the other hand, B3LYP does not describe properly the auriphilic attraction, which is manifested in very large Au–Au distances for $n = 2-4$: 480, 431

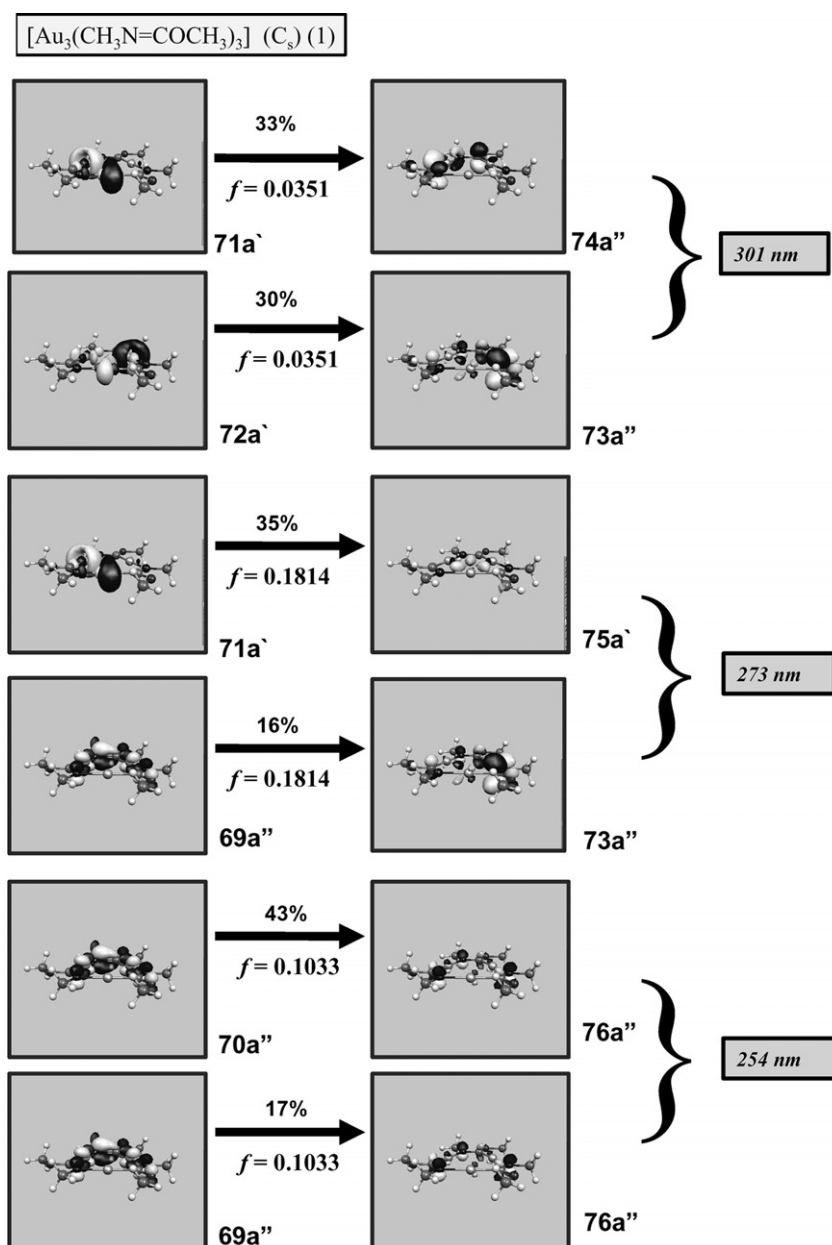


Fig. 2. The active molecular orbitals in the $[\text{Au}_3(\text{CH}_3\text{N}=\text{COCH}_3)_3]$ (**1**) electronic transitions at the PBE level.

and 405 pm, respectively. Using the PBE method we find an intermediate situation. The closest Au–Au distances in the 2–4 models are 363, 384.3 and 369.3 pm. These results must be analyzed with caution, since DFT calculations do not describe appropriately the aurophilic attraction, although they can reproduce the metallophilic distance in some occasions [17,27].

We have estimated the intermolecular interaction and aurophilic attraction energies for model 2 with counterpoise correction (CP) for the basis set superposition error (BSSE). The results for the model are shown in Table 2. The model produces an attraction at the MP2 and PBE levels. If the interaction energy, $V(R_c)$, is divided by the number of closest Au–Au contacts present in the model, pairwise energies of -25.3 and -1.8 kJ/mol are found at the MP2 and PBE levels, respectively. The MP2 magnitude is within the theoretical range, while that of PBE is poor. Perhaps for the last method, the ligands can establish an attraction. At the HF and B3LYP levels the interaction energies are positive, i.e., repulsive.

3.2. Time-dependent (TD)-DFT calculations

We calculated the allowed spin singlet transition for these systems, based on the ground state structures of models 1–4 at the PBE and B3LYP levels. Only singlet–singlet transitions were considered in these quasi-relativistic calculations. Here, we consider as permitted transitions those whose oscillator strength is different from zero. The allowed transitions obtained are shown in Tables 3 and 4. The active molecular orbitals (M.Os) in electronic transitions at the PBE level are shown in Figs. 2–4.

$[\text{Au}_3(\text{MeN}=\text{COMe})_3](1)$. The experimental evidence shows that in solution the complex is dominated by monomers. Thus, the gold–gold intermolecular interactions are not expected to be relevant in determining the electronic structure. The electronic structure of the complex has been described with two absorption peaks at 250 and 265 nm, and a weak tail at 285 nm, assigned to individual states

of a metal-to-ligand and metal-to-metal charge transfer (MLCT and MMCT) [18,21].

The theoretical calculations are described in Table 3 at the PBE level. The calculated spectrum shows three principal transitions at 254, 273 and 301 nm, matching the experimental transitions described previously. At the theoretical level, the bands are a mixture of excitations. The transition at 301.1 nm is composed mainly by $71a'(s+dz^2) \rightarrow 74a''(\pi^*)$ and $72a'(s+dz^2) \rightarrow 73a''(\pi^*)$. This band corresponds to MLCT. The second transition at 272.6 nm has one principal excitation $71a'(s+dz^2) \rightarrow 75a'(s+p)$ which is associated with MMCT. There are two secondary transitions, $69a'' \rightarrow 73a''$ and $69a'' \rightarrow 76a''$, associated with LLCT ($\pi \rightarrow \pi^*$). The third transition at 254.4 nm shows a component of greater weight $70a''(s+d) \rightarrow 76a''(\pi^*)$ of the MLCT type, while there are two smaller components of the LLCT type. The active molecular orbitals in the electronic transition are shown in Fig. 2.

The TD-DFT/B3LYP excitation for the same model is given in Table 4. The transitions are the same as those described above, but displaced to shorter wavelengths. In qualitative terms, they are practically the same as in the analysis carried out with the PBE methodology (not shown here). Sansores et al. used the B3LYP method and reported three analogous transitions: 201, 197 and 187 nm [22]. The difference with our results can be due to the fact that they used a LANL2DZ basis and pseudo-potential for gold. On the other hand, Wu et al. reported an MP2/CIS calculation for model 1 and found two transitions at 199 and 193 nm. These results showed that the charge transfers of the excitations take place mainly between the gold atoms within the Au_3 core [23].

$[\text{Au}_3(\text{MeN}=\text{COMe})_3]_n(2-4)$. When we used models 2–4, we observed a red shift of the excited bands and an increase in the transition intensity reflected in the magnitude of the oscillator strength at the PBE level (see Table 3). The bands are mainly a double MLCT of type $s+dz^2 \rightarrow \pi$, which can be understood from the M.Os shown in Figs. 3 and 4. A progressive shift in the

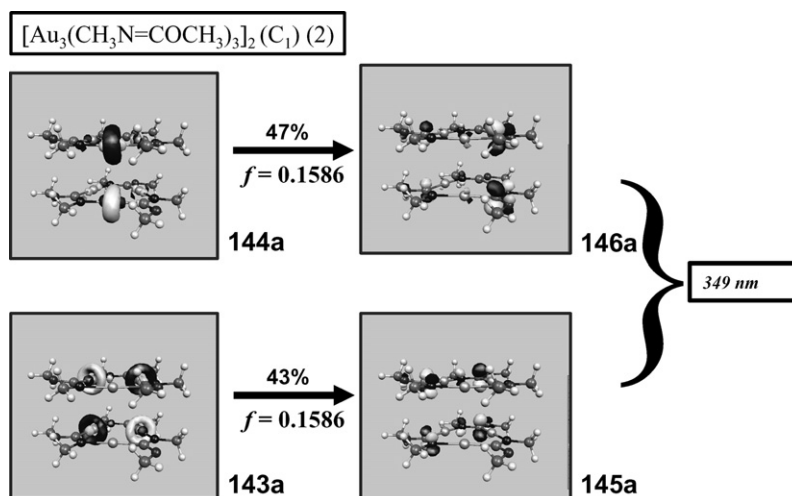


Fig. 3. The active molecular orbitals in the $[\text{Au}_3(\text{CH}_3\text{N}=\text{COCH}_3)_3]_2$ (2) electronic transitions at the PBE level.

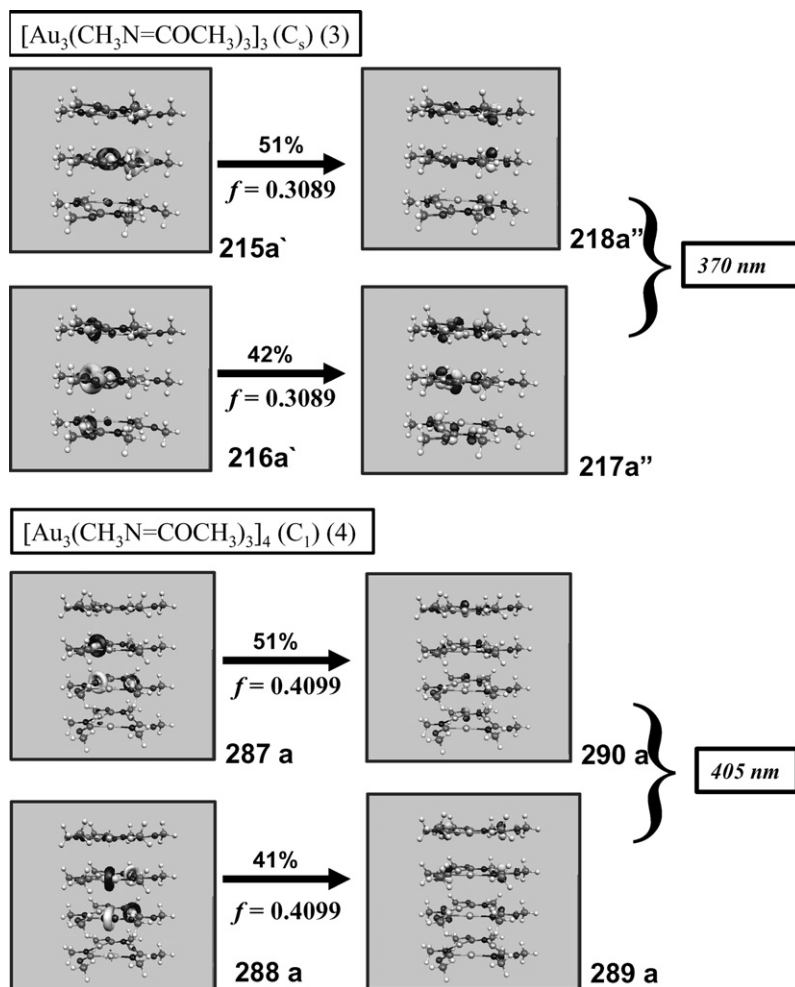


Fig. 4. The active molecular orbitals in the $[\text{Au}_3(\text{CH}_3\text{N}=\text{COCH}_3)_3]_3$ (3) and $[\text{Au}_3(\text{CH}_3\text{N}=\text{COCH}_3)_3]_4$ (4) electronic transitions at the PBE level.

wavelength of the excitation band from 349 nm ($n = 2$) to 405 nm ($n = 4$) took place by increasing the number of molecular units in the models. There is excellent agreement with the experimental solid state spectra (380 nm). When the unoccupied orbitals are analyzed, we found a π bonding character among the neighboring molecular units.

When we used the B3LYP method we found that the red shift is less noticeable (see Table 4). In qualitative terms, the orbitals involved in the transitions are of the same type as those obtained by the PBE methodology. The difference between both methods is due to the fact that in the models with B3LYP the intermolecular distances are substantially larger. This is manifested by shorter wavelengths of 272 nm ($n = 2$) to 290 nm ($n = 4$).

4. Conclusion

This study provides further information on the nature of the gold–gold intra- and intermolecular interactions in the $[\text{Au}_3(\text{MeN}=\text{COMe})_3]$ complex and on its spectroscopic properties. The idea was to show that it is possible to describe such properties through the clusters with several molecular units. Theoretical calculations at the MP2 level

are in agreement with experimental geometries and aurophilic attraction, and to a smaller extent for PBE. On the other hand, TD-DFT/PBE calculations clearly match the experimental excitation spectra. They show that intermetallic interactions are mainly responsible for the MMCT in model 1, and they also present an LLCT component which can not be neglected. In models 2–4, there is a strong dependence between the intermolecular gold–gold contact in each system and the MLCT band, evidenced by a red shift effect at the experimental solid state level.

Acknowledgements

This work was financed by FONDECYT through Project 1060044 (Conicyt-Chile) and by MIDEPLAN through the Millennium Nucleus for Applied Quantum Mechanics and Computational Chemistry P02-004-F.

References

- [1] W.-F. Fu, K.-C. Chan, V.M. Miskowski, C.-M. Che, *Angew. Chem., Int. Ed.* 38 (1999) 2783.
- [2] K.H. Leung, D.L. Phillips, M.C. Tse, C.-M. Che, V.M. Miskowski, *J. Am. Chem. Soc.* 121 (1999) 4799.

- [3] K.H. Leung, D.L. Phillips, Z. Mao, C.-M. Che, V.M. Miskowski, C.-K. Chan, *Inorg. Chem.* 41 (2002) 2054.
- [4] C.-M. Che, H.-L. Kwong, C.-K. Poon, *J. Chem. Soc., Dalton Trans.* (1990) 3215.
- [5] E. Cheng, K.-H. Leung, V.M. Miskowski, V.W.-W. Yam, D.L. Phillips, *Inorg. Chem.* 39 (2000) 3690.
- [6] T.M. McCleskey, H.B. Gray, *Inorg. Chem.* 31 (1992) 1733.
- [7] C.-M. Che, H.-L. Kwong, V.W.-W. Yam, K.-C. Cho, *J. Chem. Soc. Chem. Commun.* (1989) 885.
- [8] P.J. Costa, M.J. Calhorda, *Inorg. Chim. Acta* 359 (2006) 3617.
- [9] P. Pyykkö, *Angew. Chem., Int. Ed. Engl.* 43 (2004) 4412.
- [10] P. Pyykkö, F. Mendizabal, *Inorg. Chem.* 38 (1998) 3018.
- [11] P. Pyykkö, *Angew. Chem., Int. Ed. Engl.* 41 (2002) 1001.
- [12] H.-X. Zhang, C.-M. Che, *Chem. Eur. J.* 7 (2001) 4887.
- [13] Q.-J. Pan, H.-X. Zhang, *Eur. J. Inorg. Chem.* (2003) 4202.
- [14] E.J. Fernández, M.C. Gimeno, A. Laguna, J.M. López-deLuzuriaga, M. Monge, P. Pyykkö, D. Sundholm, *J. Am. Chem. Soc.* 122 (2000) 7287.
- [15] E.J. Fernández, P.G. Jones, A. Laguna, J.M. López-de-Luzuriaga, M. Monge, J. Pérez, M.E. Olmos, *Inorg. Chem.* 41 (2002) 1056.
- [16] E.J. Fernández, A. Laguna, J.M. López-de-Luzuriaga, F. Mendizabal, M. Monge, M.E. Olmos, J. Pérez, *Chem. Eur. J.* 9 (2003) 456.
- [17] F. Mendizabal, C. Olea-Azar, R. Briones, *Theochem* 764 (2006) 187.
- [18] J.C. Vickery, M.M. Olmstead, E.Y. Fung, A.L. Balch, *Angew. Chem., Int. Ed. Engl.* 36 (1997) 1179.
- [19] L.H. Gade, *Angew. Chem., Int. Ed. Engl.* 36 (1997) 36, 1171.
- [20] R.L. White-Morris, M.M. Olmstead, S. Attar, A.L. Balch, *Inorg. Chem.* 44 (2005) 5021.
- [21] E.Y. Fung, M.M. Olmstead, J.C. Vickery, A.L. Balch, *Coord. Chem. Rev.* 171 (1998) 151.
- [22] L.E. Sansores, R. Salcedo, H. Flores, A. Martinez, *Theochem* 530 (2000) 125.
- [23] M. Zhang, C. Mang, K. Wu, *Theochem* 759 (2006) 35.
- [24] J.P. Perdew, K. Burke, M. Ernzerhof, *Phys. Rev. Lett.* 77 (1996) 3865.
- [25] Y.-B. Wang, Z. Lin, *J. Am. Chem. Soc.* 125 (2003) 6072.
- [26] E.R. Johnson, G.A. DiLabio, *Chem. Phys. Lett.* 419 (2006) 333.
- [27] M.P. Johansson, D. Sundholm, J. Vaara, *Angew. Chem., Int. Ed. Engl.* 43 (2004) 2678.
- [28] R. Bauernschmitt, R. Ahlrichs, *Chem. Phys. Lett.* 256 (1996) 454.
- [29] M.E. Casida, C. Jamorski, K.C. Casida, D.R. Salahub, *J. Chem. Phys.* 108 (1998) 4439.
- [30] L. Olsen, P. Jørgensen, in: D.R. Yarkony (Ed.), *Modern Electronic Structure Theory*, vol. 2, World Scientific, River Edge, NJ, 1995.
- [31] R. Ahlrichs, M. Bär, M. Häser, H. Horn, C. Kölmel, *Chem. Phys. Lett.* 162 (1989) 165.
- [32] D. Andrae, U. Häusserman, M. Dolg, H. Stoll, H. Preuss, *Theor. Chim. Acta* 77 (1990) 123.
- [33] A. Bergner, M. Dolg, W. Küchle, H. Stoll, H. Preuss, *Mol. Phys.* 80 (1993) 1431.
- [34] S. Huzinaga, *J. Chem. Phys.* 42 (1965) 1293.
- [35] K. Eichkorn, O. Treutler, H. Öhm, M. Häser, R. Ahlrichs, *Chem. Phys. Lett.* 240 (1995) 283.